Investigation on Simulation of Buckling of Aluminium Sheet Alloys

Ralf Schleich[1], Christoph Albiez[2], Apostolos Papaioanu[3],
Prof. Dr. M. Liewald MBA[3]

[1] HochschulInstitute Neckarsulm, Gottlieb-Daimler-Str. 40, 74172 Neckarsulm, Germany
[2] AUDI AG, Postfach 1144, 74148 Neckarsulm, Germany
[3] Institut für Umformtechnik, Universität Stuttgart, Holzgartenstr. 17, 70174 Stuttgart, Germany

Summary:

The lack of accuracy of buckling prediction in forming simulation is widely known. This is mainly caused by insufficient element stiffness as well as a very simplified strain path but not sheet thickness dependent buckling criterion. Within this contribution a methodology for investigating such issue is developed. This paper also reveals possibilities concerning an experimental analysis of buckling sensitivity of AA6016 aluminium sheet metal alloys. For this purpose, specimen shape referring to Yoshida which cannot be used for aluminium alloys have been enhanced simulatively. Thus, nine geometries ensuring different strain paths have been developed and validated experimentally. Based on this simulative and experimental test set up a buckling criterion for plane aluminium sheets under uniaxial tension is given here.

Keywords:

Sheet Metal Forming of aluminium, buckling, wrinkles (2nd order), Yoshida-Test, forming simulation, wrinkle detection

1 Introduction

Nowadays, ensurance of surface quality of deep drawn car body parts gains additional importance for car body production. In consequence of increasing customer demands, legislative regulation concerning fuel consumption as well as additional demands of crash resistance capability measures concerning light weight materials and constructions are accretively considered as applicable for series production [1]. Within this development sheet metals with increased tensile strength and reduced sheet thicknesses simultaneously are used. Thus, the loss of geometrical moment of inertia and the decreased critical buckling load will lead to additional demands of accuracy in forming simulation. Small amounts of internal as well as external superposed lateral pressure can lead to 2nd order wrinkles at deep drawing, buckling at part handling and surface defects in consequence of thermal expansion.

This paper deals with analysis of former investigations concerning the experimental and simulative appearance of surface defects for steel materials and reveals possibilities of an enhanced analysis of buckling sensitivity of AA6016 aluminium sheet metal alloys. Former investigations have revealed tremendous insufficiencies of the so-called “Formability Plot” (see Fig. 1). Within this approach a strain path dependent criterion is defined as critical concerning wrinkles (see Fig. 2). Furthermore, significant surface defects can obviously be detected because of short-waved deflection from CAD data.

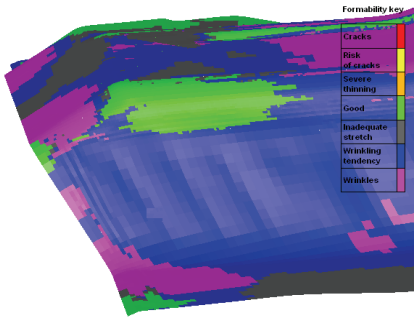

Figure 1: Formability Plot of a deep drawn part indicating critical part areas regarding wrinkles and surface defects

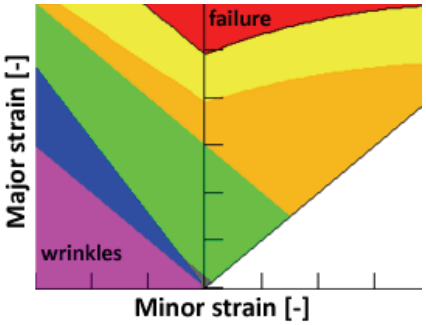

Figure 2: Simplified FLD revealing of zones due to risk of material failure and wrinkling

2 Theory

Buckling sensitivity of a deep drawn car body part consists of buckling resistance and buckling stiffness. The buckling stiffness describes resistance against first elastic deformation. The stiffness depends on sheet thickness, Young’s modulus, part geometry and state of stress. Furthermore, the buckling resistance describes resistance against a plastic deformation. Whereas both static as well as dynamic buckling resistance can be differentiated. The yield strength as well as the hardening exponent are the most relevant material parameters for a sensitive characterisation of buckling resistance. Therefore, it is obvious that strengthening procedures like an additional aging or a defined pre-stretching show a positive effect concerning initiation of buckling [2]. Hence, buckling is initiated by a material specific buckling sensitivity due to plate stiffness as well as the respective state of stress.

Analogous to buckling of beams, buckling of thin sheet metals may also occur under a compression load. For determination of lateral forces and moments the conventional plate theory is assumed within this investigation. This approach only describes buckling under a compression orthogonal to the middle plane. In case of wrinkles of 2nd order this assumption is insufficient because critical buckling loads occur in plane. With indirect integration and further parameter adjustments this approach can be adapted for deep drawing [3]. Furthermore, buckling of sheet metals may occur under an uniaxial tension load. Under certain circumstances buckles can be initiated because of lateral contraction. An experimental validation of such theories can be gained by stretching thin sheet metal strips with a length to width ratio bigger than 5 [4]. Such strips are clamped at the short side and uniaxially stretched. Large tension stresses are necessary next to the clamping to realise shear in outer regions of the strip. These lateral tension stresses lead to a moment which leads to a negative deflection in the middle of the strip.

Thus, lateral compression stresses are necessary for unbending the sheet. According to these assumptions shear stresses occur due to lateral compression. As consequence of change of sign of lateral stresses the sign of shear stress will change, too. Former research activities of [4] have shown the dependency of buckling sensitivity and blank size. Furthermore, the current state of stress also effects the initiation and shape of bifurcation as well [5].

At conventional deep drawing processes a combination of several states of stress occurs. The impact of blank geometry which is relevant for such kind of forming processes was experimentally investigated und analysed by [6]. Further investigation at the Institute for Metal Forming Technology has shown a dependency of buckling on the sheet thickness [7].

A reproducable test procedure for investigating impact of material parameters for steel alloys on buckling was developed by [8]. Within this work a specimen which produces an additional geometry caused contraction under uniaxial tension is shown (see Fig. 4). The amount of geometry caused contraction leads to buckling of steel alloys. The use of Aluminium will lead to strain localisation in flange till material failure without significant buckling.

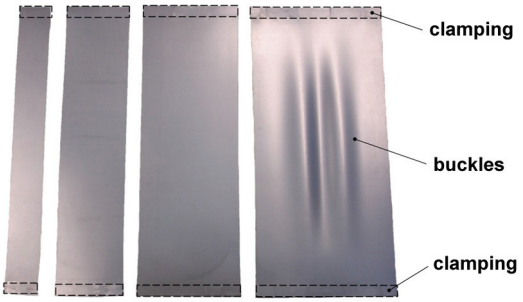

Figure 3: Evolution of wrinkles due to transversal contraction at uniaxial tension [7]

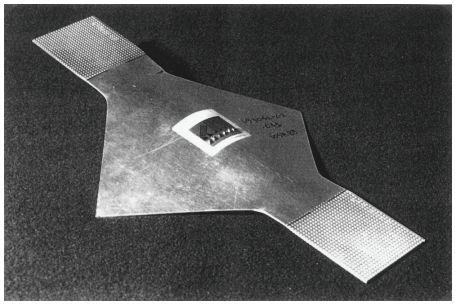

Figure 4: Tested Yoshida-specimen [8]

3 Simulative development of a buckling geometry under uniaxial tension for aluminium alloys

The simulation of buckling geometry according [8] under an uniaxial tension load with the material properties of an AA6016 aluminium alloy and the sheet thickness of 1.04mm reveals a strain localisation until necking in flange without a significant buckling tendency. Furthermore a lack of strain inducement in the middle of specimen is revealed. Thus, the following specimen geometries have been modified the way that the corners of the middle section have been chamfered to reduce notch effects. The middle section which is superposed by additional lateral contraction is convex chamfered to gain a homogenised stress allocation. By the simulative investigation of uniaxial tension of several buckling geometries nine shapes with different buckling sensitivities have been derived. For this purpose the length and width is alternated to realise different state of stresses and load paths. Fig. 5a-i shows the developed and realised geometries concerning the initiation of buckling under uniaxial tension.

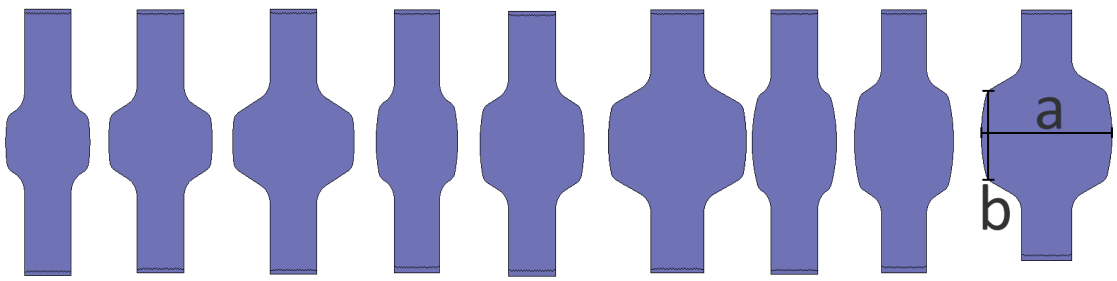

Figure 5: a-i) Shapes of specimen for investigating buckling behaviour of aluminium sheet metal

Thus, an investigation concerning a compression stress evolution by time can be done. Fig. 6 shows an exemplary sequence of a compression stress simulation of geometry 8065 for an AA6016 aluminium alloy under uniaxial tension. Starting with the unstrained specimen in Fig. 6a first compression stresses evolute in the middle region (see Fig. 6b). In the following states a localisation of compression stresses in the middle proceeds (see Fig. 6c) until the point of bifurcation is reached. Then a change of sign occurs to positive tension stresses (see Fig. 6d).

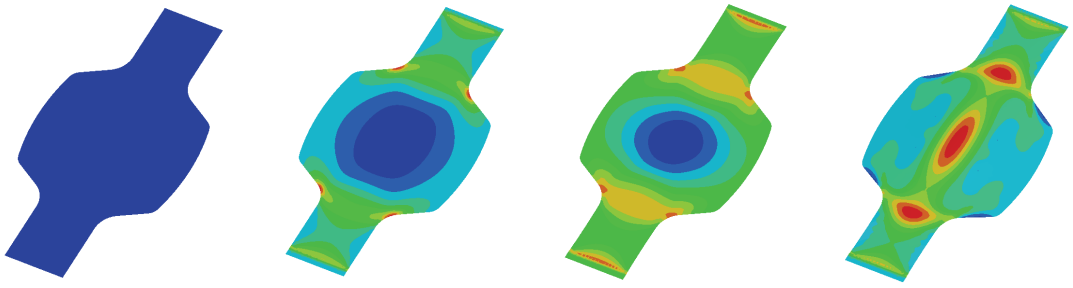

a b c d

Figure 6: Visualisation of lateral compression (specimen 8065): a) initial (t=0); b) first lateral compression (t=0,1); c) localisation of transversal compression (t=0,26); d) buckling und inversion of stress (t=0,31)

This evolution of compression stresses also can be quantitatively investigated. Fig. 7 shows the evolution of compression stresses by time for all investigated shapes of specimen. The respective change of sign indicates the moment of bifurcation. Thus, it can be shown that specimens with a length of 40mm and a width of 45mm and 55mm do not show any buckling tendency at all. All remaining geometries show the intended buckling behaviour which is induced by the change of sign of stress. Furthermore, an increase of width leads to an accelerated bifurcation. For example, the investigation of specimen shape 8055 reveals the correlation of lateral compression stress and buckling height (see Fig. 8). The increase of lateral compression stresses evolutes progressive and non-linear by time until buckling occurs.

Further investigation of buckling height shows an opposite orientation in moment of bifurcation as realised later on. With further straining and a further decrease till change of sign of lateral contraction the final orientation of buckle height is reached. Thus, the phases of buckling development can be separated into so called stable and unstable buckling.

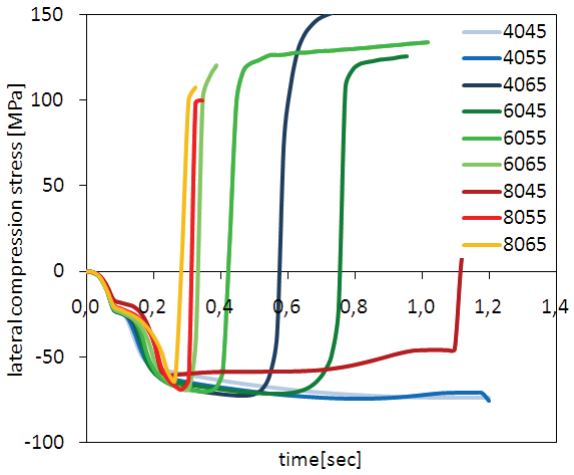

Figure 7: Analysis of lateral compression of investigated specimens

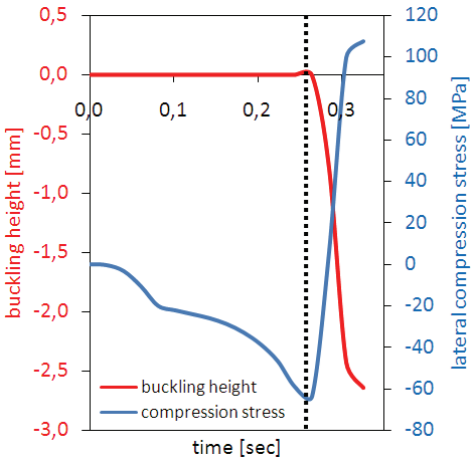

Figure 8: Evolution of buckling height and lateral compression of specimen 8055

In the following the critical buckling load will be investigated separately. Fig. 9 reveals that for different width and length values bifurcation is always initiated at the same compression stress value. Such critical compression stress value is also reached at the same B/A-ratio of 1.6. Thus, the initiation of bifurcation is dependent on the allocation of local compression stress and less on size of the sheet.

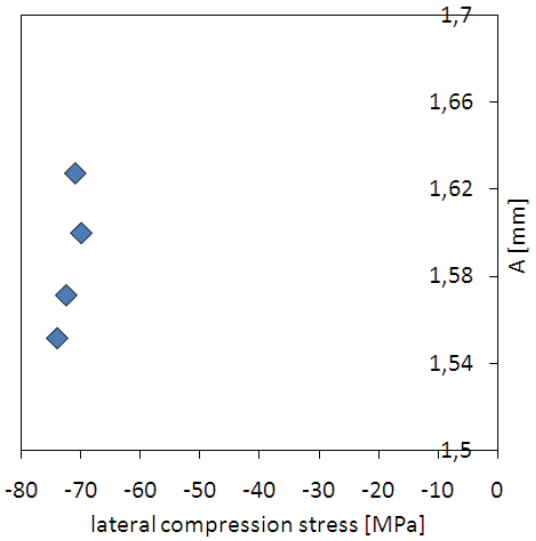

Figure 9: Evolution of critical transversal compression vs. width A

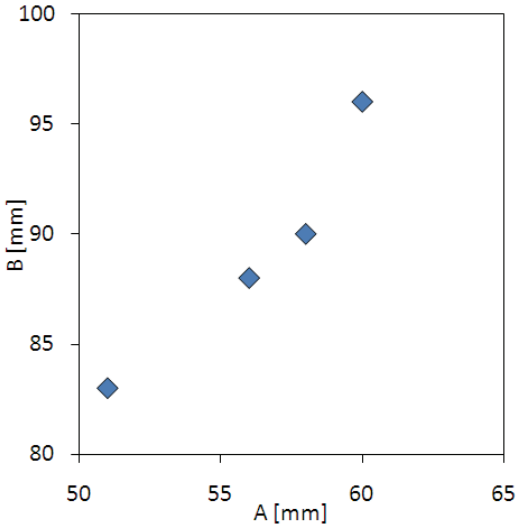

Figure 10: Specimens for investigating buckling of aluminium sheet metal

4 Experimental investigation

Based on the geometries developed before an experimental test series is arranged. The nine shapes of specimen will be water cutted and prepared for in-situ forming analysis. The optical forming analysis is based on principals of photogrammetry. For this purpose, a definite identification of each measurement point is urgently needed. Therefore, a stochastic pattern with clear black/white contrasts is applied and digitised. After that the specimen will be optically tracked with 12 frames per second at a uniaxial forming speed of 20mm/min. To improve reproducibility a maximal stroke limitation of 15mm is used. Thus, a strain superposition can be visualised for each frame as well as an analysis over time can be done.

Results concerning a strain- and displacement analysis will be discussed in the following. Fig. 11 shows the measured buckle height after bifurcation. The geometry 4045 shown below reaches a buckling height of 6mm.

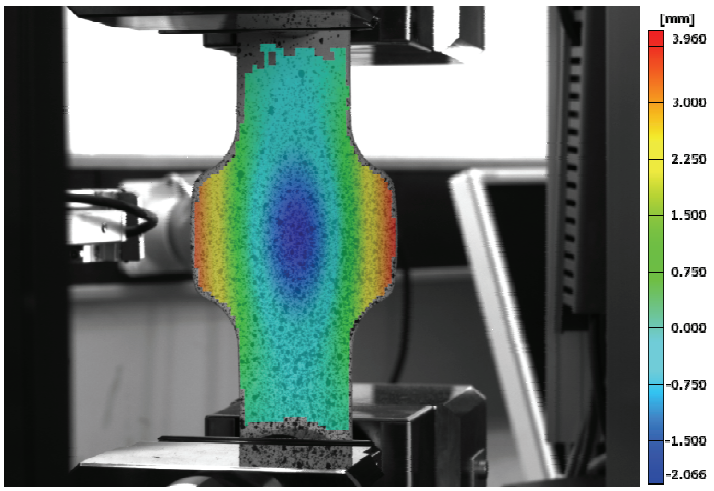

Figure 11: In-situ forming analysis of 4045 buckling specimen indicating wrinkling height; AA6016 material

Furthermore, the optical forming analysis offers the possibility of a space-resolved analysis of strain distribution over time. The major strain components can be investigated as well as the equivalent strain (see Fig. 12 and Fig. 13). By linking the forming analysis with the internal force measurement, the stress distributions can also be visualised. However, this was not realised within this investigation.

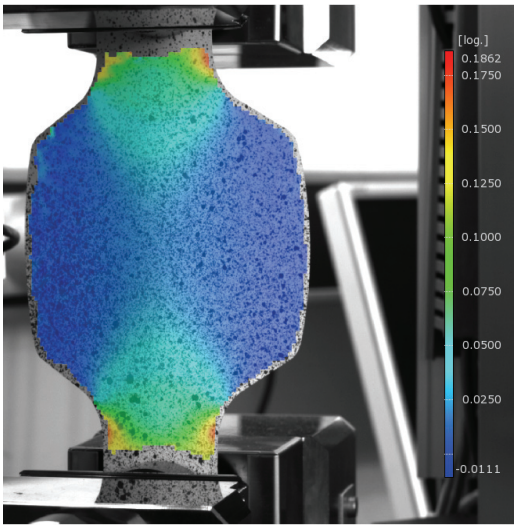

Figure 12: Visualisation of major strain of 8065-buckling specimen under uniaxial tension after bifurcation (AA6016)

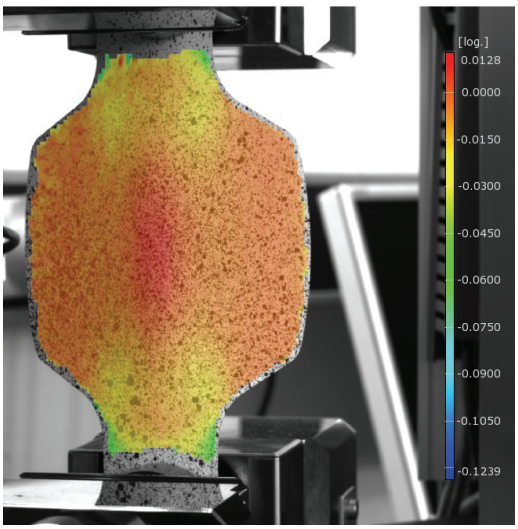

Figure 13: Visualisation of minor strain of 8065-buckling specimen under uniaxial tension after bifurcation (AA6016)

The comparison of respective buckling heights shown in Fig. 14 and Fig. 15 reveals a significant dependency to the specimen shape. At a constant width the buckling height increases with a higher length. The specimen with geometry 8065 exhibits a 3.3mm higher buckling height than the geometry 4065.

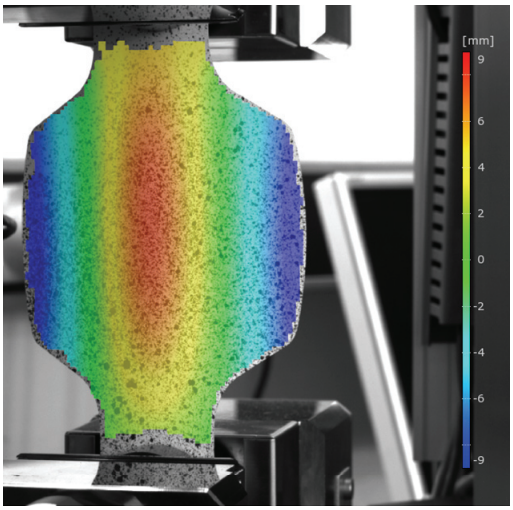

Figure 14: Visualisation of wrinkling height of 8065-buckling specimen under uniaxial tension after bifurcation (AA6016)

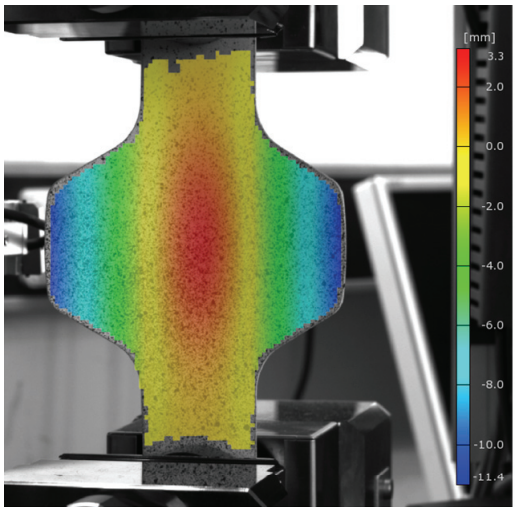

Figure 15: Visualisation of wrinkling height of 4065-buckling specimen under uniaxial tension after bifurcation (AA6016)

Furthermore, the force-stroke-curves can be used for detection and characterisation of buckling behaviour of sheet metals under uniaxial tension. The comparison of several specimen lengths (see Fig. 16) reveals that with increasing length less drawing force is needed. The maximal difference reaches a value up to 250N. Some of these geometries show a discontinous evolution in the force-stroke-diagram in moment of bifurcation. Thus, the derivation due to stroke shows a minimum at that moment (see Fig. 17). Hence, a distinct criterion to determine the moment of bifurcation can be defined.

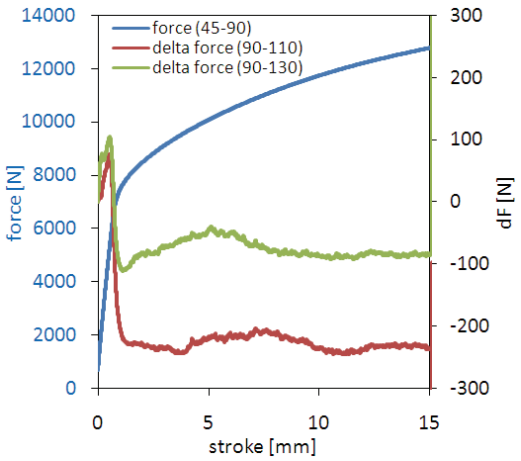

Figure 16: Force-stroke-diagram of several specimen geometries under uniaxial tension

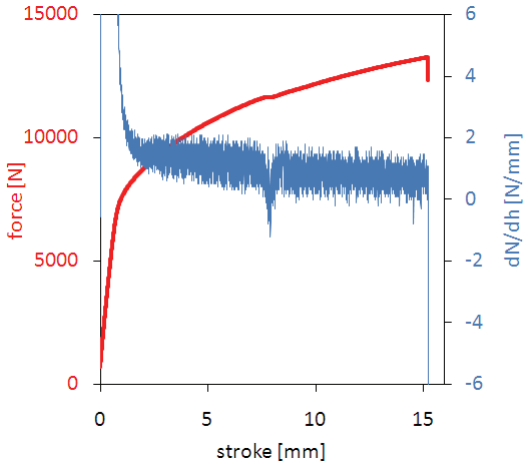

Figure 17: Force-stroke-diagram and derivation of force for indication of bifurcation

Initiation of bifurcation can be separated into stable and instable phase as described before. The analysis of stroke distance at initiation of stable buckling, shown in Fig. 18, reveals a direct correlation of specimen geometry and moment of bifurcation. The investigation of geometry 8065 shows a stable buckling already at a stroke of 1mm. Geometry 6045 exhibits a buckle after a stroke of 4mm. Fig. 19 reveals the correlation between stroke and specimen geometry. The correlations found within this investigation reveal a comparable tendency of buckle initiation as shown for the stable bifurcation. The first buckle is initiated at a stroke of 2mm for geometry 8065 and the last one is initiated at a stroke of 5.5mm for geometry 4045.

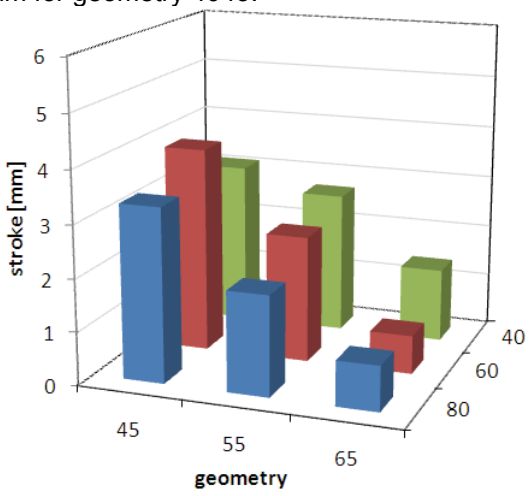

Figure 18: Stroke at initialisation of stable bifurcation for AA6016

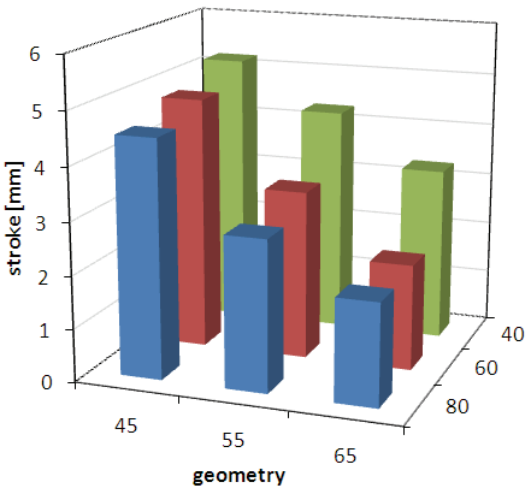

Figure 19: Stroke at initialisation of unstable bifurcation for AA6016

5 Conclusion

Although the experimental investigation also shows the buckling behaviour as seen in simulation, the moment of buckling as well as the buckling height could not be predicted. Geometries 4045 and 4055, which could not be stretched until buckling because of material failure, also have shown a buckle height of 6mm in experimental tests. Furthermore, based on the conventional forming limit plot, first occurrence of buckling or wrinkling could not be predicted at all for these buckling geometries. Thus, this investigation reveals that wrinkles of 2nd order cannot be predicted for all cases. Nevertheless the investigation concerning initiation of first buckles shows the correlation to the allocation of lateral compression stress ratio of 1.6 which is validated by [4] and [8].

The in-situ forming analysis also reveals the phases of stable and unstable buckling. The direction of stable buckling must not be identical to the direction of unstable buckling. Furthermore the force-stroke-diagram clearly indicates moment of buckling, thus the critical buckling load can be detected.

This contribution also reveals potentials concerning an investigation of a buckling criterion for deep drawing as well as for external load conditions. Future works will have to concentrate on investigating further impact parameters as well as on the improvement of buckling prediction in Finite-Element-simulation.

6 Literature

[1] Liewald, M., Schleich, R.: *Robust Processes in Sheet Metal Forming in Car Body Manufacturing with Regard to Production Volume*; Key-Note-Vortrag IDDRG 2007 Konferenz Györ, 2007

[2] Wallentowitz, H.; *Strukturentwurf von Kraftfahrzeugen, Vorlesungsumdruck*, 3. Auflage, fka – Forschungsgesellschaft Kraftfahrwesen mbH Aachen, Aachen, Februar 2006

[3] Klein, B.: *Leichtbaukonstruktion*, Vieweg Verlag, Wiesbaden 1994.

[4] Friedl, N., Rammerstorfer, F. G., Fischer, F. D.: *Zum Beulen von Platten unter globalem Zug*, Zeitschrift für angewandte Mathematik und Mechanik, Nr.79, Wiley-VCH-Verlag, Weinheim 1999

[5] Grote, H.: *Zum Einfluss des Beulens auf die Tragfähigkeit von Walzprofilen aus hochfestem Stahl*, Dissertation, Ruhr-Universität Bochum, Fakultät für Bauingenieurwesen, 2003

[6] Bräunlich, H., Lailach, A.: *Verbesserung der Bauteilqualität durch Streckziehen*, Blech Rohre Profile, 40 Nr.6, Meisenbach Verlag, Bamberg, 1993

[7] Vlahovic, D., Schleich, R., Liewald, M.: *Beulen von Feinblechen unter einachsiger Zugbeanspruchung*; UTF-Science; Meisenbach Verlag, 2008

[8] Yoshida, K., Hayashi, J., Niyauchi, K., Hirata, M., Hira, T., Ujihara, S.: *Assessment of Fitting Behavior and Shape Fixation by Yoshida Buckling Test - A Way to Overall Formability*, International Symposium on New Aspects of Sheet Meta